

# Central European Journal of Chemistry

DOI: 10.2478/s11532-007-0003-2 Research article CEJC 5(2) 2007 516-535

# Comparative study of layered tetravalent metal phosphates containing various first-row divalent metals. Synthesis, crystalline structure

László Szirtes<sup>1\*</sup>, László Riess<sup>1</sup>, János Megyeri<sup>1</sup>, Ernő Kuzmann<sup>2</sup>

<sup>1</sup> Institute of Isotopes, Hungarian Academy of Sciences, H-1525 Budapest, Hungary

<sup>2</sup> Research Group of Nuclear Methods in Structural Chemistry, Department of Nuclear Chemistry, HAS, Eötvös Lóránd University, H-1518 Budapest, Hungary

Received 15 June 2006; accepted 15 November 2006

Abstract: The transition metal forms of  $\alpha$ -zirconium-. titanium-, and hafnium phosphates were prepared by ion exchange method. Their structure was investigated by X-ray powder diffraction (XRPD) method. It was found that the transition metal containing phosphates have the same layered structure as the pristine tetravalent metal phosphates, except for the increase of interlayer distance from 7.6 Å to  $\sim 9.5$  Å. As a result of the incorporation of transition metals in the layers, the c-axis is increased from  $\sim 15$  Å to  $\sim 20$  Å (in the case of titanium phosphate to  $\sim 25$  Å). All other parameters (a, b and  $\beta$ °) are practically unchanged.

© Versita Warsaw and Springer-Verlag Berlin Heidelberg. All rights reserved.

Keywords: Ion exchange, XRPD analysis

#### 1 Introduction

The phosphates of tetravalent cations, such as Sn, Ti and Zr were synthesised in the end of  $19^{th}$  century. However, the real interest in this subject (because of their good resistance against radiation) began since the 1950s in connection with their possible use in radio-chemical processes. The literature in this field is very rich. Monographs on tetravalent metal phosphates were published both by Tanaev [1] and Averbuch [2]. Many layered

<sup>\*</sup> E-mail: szirtes@iki.kfki.hu

tetravalent metal phosphates have been characterised by X-ray method. According to these investigations it became clear that two stable layers exist, corresponding to the  $\alpha$ -and  $\gamma$ - structure. The structure of  $\alpha$ -zirconium phosphate (hereafter ZrP) was found to be a layered monoclinic one, as determined first by Clearfield [3, 4] and investigated by other authors [5, 6]. Nowadays, the structure is clear; the data are widely known and used.

The structure of  $\alpha$ -titanium phosphate (hereafter TiP) was found to be iso-structural with that of  $\alpha$ -ZrP, as became clear in the mid 1990s from the more detailed study of Bruque et al. [7].

The  $\alpha$ -hafnium phosphate (hereafter HfP) was first prepared by Clearfield [8]. Later on, Tomita et al. [9] prepared it by refluxing freshly formed amorphous HfP in H<sub>2</sub>PO<sub>4</sub> at the boiling point for more than 210 hours. In the mid 1980s, HfP was also prepared by us using the fluorine-complex method and the structure of crystalline  $\alpha$ -HfP was investigated [10].

Later, the  $\alpha$ - and  $\gamma$ -zirconium and titanium phosphates were extensively studied, and have been reviewed by Clearfield [11] and other authors [12–14], respectively. Later, an interest arose in nanoparticles ( $\gamma$ -ZrP/Si) and transition metal salts (i.e. ZrMnHPO<sub>4</sub> and others) [15, 16] used for catalytic and other purposes. A classification of these phosphates is given by Brandel and Dacheux [17].

Shaksooki et al. [18] and the current authors have earlier [19–21] proposed that the layered hafnium phosphate ( $\alpha$ -HfP) isomorphous with the  $\alpha$ -zirconium phosphate because their thermal-, ion exchange, and some other properties were found to be very similar. Detailed structural data of hafnium phosphate ( $\alpha$ -HfP) and related intercalates are also reviewed by Suárez et al. [22].

In this paper, we summarise the results of recent investigations on the crystalline structure of the first-row transition metal containing  $\alpha$ -zirconium-, titanium- and hafnium phosphates in comparison with their pristine tetravalent metal phosphates.

# 2 Experimental

#### 2.1 Synthesis

All chemicals used were analytical grade.

The  $\alpha$ -zirconium-, titanium-, and hafnium phosphates were prepared via the fluorocomplex, as first proposed by Alberti and Torracca [5].

A typical process used for  $\alpha$ -zirconium phosphate was; 27.5 g of ZrOCl<sub>2</sub>.8H<sub>2</sub>O was dissolved in 400 cm<sup>3</sup> de-ionised water, then 20 cm<sup>3</sup> of HF (40% solution) was added and the mixture was heated at 80 °C. At this temperature (with constant vigorous stirring) 230 cm<sup>3</sup> solution of 11.9 M H<sub>3</sub>PO<sub>4</sub> was added very slowly. After that, the solution was allowed to stand at 80 °C (with stirring and at constant solution level) for 24 hours to evaporate the fluorine. The resulting precipitate was then washed with de-ionised water until it reached pH $\cong$ 4 and dried over P<sub>2</sub>O<sub>5</sub> in a dessiccator.

In the case of  $\alpha$ -titanium phosphate, the following typical process was used; 11.8 g of TiCl<sub>4</sub>was dissolved in 125 cm<sup>3</sup> of 3.0 M HF solution, then, 500 cm<sup>3</sup> of 6.3 M H<sub>3</sub>PO<sub>4</sub> solution was slowly added with vigorous stirring. The mixture was then allowed to stand at 60 °C (with stirring and at constant solution level) for 168 hours to evaporate the fluorine. Subsequent steps were the same as described for  $\alpha$ -ZrP.

In the case of  $\alpha$ -hafnium phosphate, typically 2 g of HfCl<sub>4</sub> was dissolved in 125 cm<sup>3</sup> of 3 M HF solution, then 500 cm<sup>3</sup> of 6.3 M H<sub>3</sub>PO<sub>4</sub> solution was added slowly with vigorous stirring. The mixture was heated to 80 °C and allowed to stand at this temperature (with stirring and at constant solution level) for 24 hours to evaporate the fluorine. The rest of the process was concordant with that for  $\alpha$ -ZrP [23].

The first-row divalent metal containing samples were prepared by the ion exchange method. A typical example of this method was the following. Three grams of freshly prepared ion exchanger ( $\alpha$ -ZrP,  $\alpha$ -TiP and  $\alpha$ -HfP, respectively) was mixed into (equilibrated) 100 cm<sup>3</sup> of 0.1 M Me(II)-acetate solution (where Me=Co, Ni, Mn, Cu and Zn, respectively). The equilibration (mixing) continued for 200 hours at 80 °C (with stirring and at constant solution level). At the end of the process, the precipitate was washed with 200 cm<sup>3</sup> of deionised water and dried in a desiccator over saturated BaCl<sub>2</sub>.

#### 2.2 Analytical

The zirconium, the titanium, the hafnium, and the phosphorous content of the given samples were determined by the spectrophotometric method as described by Sandell [24].

The Me(II) contents, both of the original and residual solutions, were determined by spectrophotometer, using a SPECTROMOM 195D type photometer. The determinations were taken at wavelength of 530, 465, 475, 545 and 530 nm, against the given standards for Co, Ni, Mn, Cu and Zn ions, respectively.

The rate of ion uptake was calculated from the difference of Me(II) content of the above solutions.

The samples were controlled by elemental (carbon) analysis to determine the presence of acetate.

#### 2.3 Identification

The samples were identified using XRPD analysis. The XRPD study was performed with a Bragg-Brentano geometry, using powder samples (pressed before into the sample holder) with a DRON-2 computer controlled diffractometer (at 45kV and 35 mA) with the  $\beta$  filtered Co<sub>K $\alpha$ </sub> radiation ( $\lambda = 1.7890 \text{Å}$ ) at 25±1 °C. The goniometer speed chosen was 1/4 °min<sup>-1</sup> in the range of 2 $\Theta$ =3-110°. To finish the data collection, the first few lines of the pattern were re-measured to control of the stability of the X-ray source. The diffraction patterns were evaluated using EXRAY peak searching software [25] and refined by Rietveld's method [26]. At least the structure of investigated samples was modelled, using "PowderCell 2.3" software [27].

During the estimation, an effect of texture on line intensity was taken into consideration.

#### 2.4 Thermal analysis

The thermal analysis was carried out using a Mettler TA1-HT computer controlled thermobalance that simultaneously provided DTA and TG data. The heating rate was 5 °C  $\rm min^{-1}$  in the temperature range of 25-1000 °C, the reference material was dehydrated  $\rm Al_2O_3$ , and Pt crucible was used in ambient air. An adequate computer program TA-E1 evaluated the DTA and TG data. The results were presented in detail in previous papers [28–30].

#### 2.5 Specific surface

This was measured by the BET method as previously descried [31].

#### 3 Results and discussion

The elemental analysis of samples gave carbon content under the detection limit; consequently it showed no acetate can be present in the synthesised materials.

On evaluating the analytical data of prepared tetravalent metal phosphates, a ratio of  $1:2 \text{ (Me/PO_4)}$  was found.

The first-row transition metals were incorporated in the tetravalent metal phosphate structures using the ion exchange method. During this process, the hydrogen atoms of phosphate groups were exchanged for transition metals. The ion uptake data found here are presented in Table 1.

Metal(IV)		Sol	lution in	$\mathrm{mM/ml}$		
		Co(II)	Ni(II)	Mn'(II)	Cu(II)	Zn(II)
	initial	0.080	0.10	0.10	0.10	0.10
$\operatorname{Zr}$	residual	0.054	0.049	0.042	0.045	0.046
	ion uptake	0.026	0.051	0.058	0.055	0.054
	in %	33	51	58	55	54
	initial	0.080	0.10	0.10	0.10	0.10
$\operatorname{Ti}$	residual	0.034	0.038	0.023	0.022	0.023
	ion uptake	0.046	0.062	0.077	0.078	0.077
	in %	58	62	77	78	77
	initial	0.080	0.10	0.10	0.10	0.10
Hf	residual	0.052	0.068	0.039	0.048	0.045
	ion uptake	0.028	0.032	0.061	0.052	0.055

32

61

52

55

35

in %

**Table 1** Analytical data of samples equilibrated during 200 hours.

Durind the experiments were found that, the ion uptake increases with increasing equilibration time. After 200 hours of digestion, the ion uptake increased very slowly, although the total (100 %) change of hydrogen atoms by first-row divalent transition metal ions could not be achieved under the given experimental conditions. Based on analytical data, the following  $\mathrm{Me^{4+}/Me^{2+}}$  molar ratios were calculated for samples equilibrated for 200 hours:

Table	<b>2</b>	Molar	ratio	of	$\mathrm{Me^{4+}}$	$/{\rm Me}^{2+}$ .
-------	----------	-------	-------	----	--------------------	--------------------

	Co(II)	Ni(II)	$\operatorname{Mn}(\operatorname{II})$	Cu(II)	$\operatorname{Zn}(\operatorname{II})$
Zr	1/0.33	1/0.51	1/0.58 1/0.77 1/0.61	1/0.55	1/0.54
Ti	1/0.58	1/0.62	1/0.77	1/0.78	1/0.77
Hf	1/0.35	1/0.32	1/0.61	1/0.52	1/0.55

According to these data the

 $Co < Ni < Mn > Cu \approx Zn (Zr)$ 

 $Co < Ni < Mn \approx Cu \approx Zn$  (Ti) and

Ni < Co < Cu < Zn < Mn (Hf)

ion uptake orders can be proposed and the following compositions are suggested:

$$\alpha$$
-**Zr**(**HPO**<sub>4</sub>)<sub>2</sub>; ZrCo<sub>0.3</sub>H<sub>1.4</sub>(PO<sub>4</sub>)<sub>2</sub>; ZrNi<sub>0.46</sub>H<sub>1.08</sub>(PO<sub>4</sub>)<sub>2</sub>; ZrMn<sub>0.49</sub>H<sub>1.02</sub>(PO<sub>4</sub>)<sub>2</sub>  
ZrCu<sub>0.54</sub>H<sub>0.92</sub>(PO<sub>4</sub>)<sub>2</sub>; ZrZn<sub>0.55</sub>H<sub>0.9</sub>(PO<sub>4</sub>)<sub>2</sub>;

$$\alpha$$
-Ti(HPO<sub>4</sub>)<sub>2</sub>; TiCo<sub>0.58</sub>H<sub>0.84</sub>(PO<sub>4</sub>)<sub>2</sub>; TiNi<sub>0.69</sub>H<sub>0.62</sub>(PO<sub>4</sub>)<sub>2</sub>; TiMn<sub>0.77</sub>H<sub>0.46</sub>(PO<sub>4</sub>)<sub>2</sub>; TiCu<sub>0.78</sub>H<sub>0.44</sub>(PO<sub>4</sub>)<sub>2</sub>; TiZn<sub>0.77</sub>H<sub>0.46</sub>(PO<sub>4</sub>)<sub>2</sub>;

$$\alpha$$
-Hf(HPO<sub>4</sub>)<sub>2</sub>; HfCo<sub>0.35</sub>H<sub>1.3</sub>(PO<sub>4</sub>)<sub>2</sub>; HfNi<sub>0.32</sub>H<sub>1.36</sub>(PO<sub>4</sub>)<sub>2</sub>; HfMn<sub>0.61</sub>H<sub>0.78</sub>(PO<sub>4</sub>)<sub>2</sub>; HfCu<sub>0.5</sub>H(PO<sub>4</sub>)<sub>2</sub>; HfZn<sub>0.55</sub>H<sub>0.9</sub>(PO<sub>4</sub>)<sub>2</sub>.

As a result of thermal treatment the DTA-TG patterns showed four endothermic processes accompanied by mass loss. From these, the first and second were identified as crystal water loss, the former slightly bonded on the surface while the latter is bonded inside the layers. The other two processes cover the structural water loss originating from the decomposition of phosphate groups going in two steps in the presence of transition metal ions. Against the patterns of pure tetravalent metal phosphates, the patterns of first-row transition metal ion containing samples showed a two-step character endotherm process.

The original tetravalent metal phosphates have *one mol* crystal water per molecule unit, while their transition metalcontaining forms have about 2.41(Co), 1.25(Ni), 1.80(Mn), 1.04(Cu) and 2.38(Zn) mole per unit molecule [28–30].

2.5

Table 3 Specific surface areas.  $\alpha$ -ZrP Co(II)Ni(II)Mn(II)Cu(II)Zn(II)0.22.3 2.5 2.5 2.5 2.5  $\alpha$ -TiP 0.3 2.6 2.6 2.6 2.6 2.6  $\alpha$ -HfP

2.6

The measured specific surface area values  $[m^2 \cdot g^{-1}]$  of Me(II) containing samples are:

They are identical within the error of measurement and about *one* order of magnitude higher than that of the original (free from transition metal ions) phosphates. The results probably can be connected with the increasing of interlayer distance after taking up the given transition metals.

2.5

2.5

2.6

#### 3.1 Crystal structure determination

0.5

Using the XRPD method, attempts were made to determine the crystal structure of the transition metal containing tetravalent metal phosphates.

#### 3.1.1 $\alpha$ -metal(IV) phosphates [M(HPO<sub>4</sub>)<sub>2.</sub> $nH_2O$ ] where M = Zr, Ti, Hf, respectively

Because of the structural data of  $\alpha$ -ZrP and  $\alpha$ -TiP are well known [4–8], we give here in more detail only results concerned to  $\alpha$ -HfP, which we did not publish (in such form) until now.

The optimum evaluation was found when the monoclinic form was considered with the  $P_{1\,2}$  space group. Taking into consideration these symmetry conditions, the XRPD pattern was calculated and compared with those obtained experimentally (50 Bragg peaks). The difference plot of  $\alpha$ -HfP is shown on Fig. 1.

Using the refined results, the cell parameters were then derived. The unit cell data were compared with those of  $\alpha$ -ZrP and  $\alpha$ -TiP, found by us earlier, and are collected in Table 4 in comparison with data of Clearfield, Bruque and Suáres [7, 8, 22], respectively. The unit cell parameters of all phosphates obtained here correspond well to those measured by other authors, as can be seen from the data of Table 4.

As it can be seen from Table 4, the unit cell parameters of samples prepared by us and by the cited authors are practically identical. In spite of the fact that in case of  $\alpha$ -HfP we used a different method of preparation as used by Suárez et al. [22].

The positional and thermal parameters of the atoms in HfP are presented in Table 5, while the selected bond distances (in Å) and bond angle data (in degrees) of all three tetra-valence metal phosphates are given in Table 6 and 7, respectively.

All atomic distances and angles and also temperature factors showed no anomalous discrepancies.

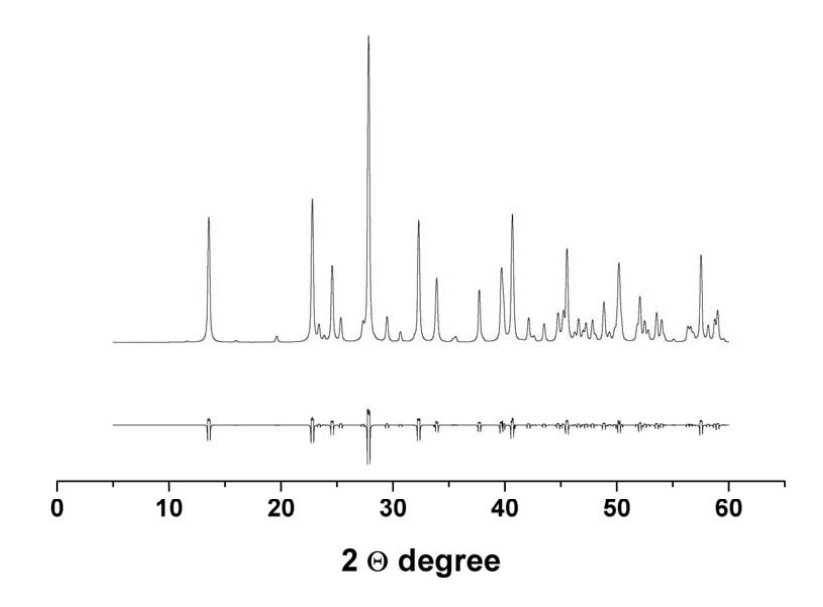


Fig. 1 The difference plot of  $\alpha$ -hafnium phosphate (measured and calculated).

	o-ZrP	α-TiP	0/-
1	able 4 Unit cen	parameters of metal(1	(v) phosphates.

	α <b>-Z</b>	ZrP	α-'	ГiР	α-	HfP
a (Å)	9.061(1)	9.060 [8]	8.638 (4)	8.6403 [7]	9.013(1)	8.9955 [22]
b (Å)	5.297(2)	5.297 [8]	5.010(4)	5.0093 [ <b>7</b> ]	5.271(2)	5.2439 [22]
c (Å)	15.415(2)	15.414 [ <mark>8</mark> ]	15.511(5)	15.5096 [ <b>7</b> ]	15.482(3)	15.4768 [22]
$eta^{\circ}$	101.71 (3)	101.7 [8]	101.3(3)	101.3 [ <b>7</b> ]	101.72(3)	101.64 [22]
$d_{002} (\mathring{A})$	7.55	7.60 [8]	7.605	-	7.5800	7.60 [22]
Vol. $(\mathring{A}^3)$	724.51 (5)	724.3 [8]	658.28(8)	-	720.22(5)	713.37 [22]
Rel. mass	1204.78	-	1031.50	-	1553.86	-
Atoms in	64.0	-	64.0	-	64.0	-
X-ray density $(g \cdot cm^{-3})$	2.7613	2.762 [8]	2.6020	-	3.5826	3.430 [22]
Mass abs. coeff. $(cm^2 \cdot g^{-1})$	97.47	-	94.47	-	132.47	-

The similarities between the new data and that already known for  $\alpha$ -ZrP shows that the  $\alpha$ -HfP structure is iso-structural with that of  $\alpha$ -ZrP. Similar to  $\alpha$ -ZrP, the metal atoms lie nearly distorted in a main plane and they are bonded by phosphate groups which are situated alternately above and below the main plane. Three oxygen atoms of each phosphate group are bonded to three different hafnium atoms forming a distorted equilateral triangle. Each hafnium atom is thus octahedrally co-ordinated by oxygens. Taking into consideration the facts written above, we assumed the existence of zeolitic type cavities similar to those which exist in the  $\alpha$ -ZrP structure. The thickness of the layer was found to be 628 pm (it was calculated using the baricentre of O atoms of P-OH groups lying on the opposite sides of a layer). The calculated free area associated with

**Table 5** The positional and thermal parameters of atoms in  $\alpha$ -hafnium phosphate

atom	X	У	Z	$\mathbf{B}_{iso}$
Hf	0.7375	0.2522	0.4855	0.0023
P1	-0.0240	0.7533	0.6120	0.0081
P2	0.5012	0.2344	0.6229	0.0081
O1	0.1235	0.8141	0.6032	0.0120
O2	-0.0833	0.4801	0.5721	0.0120
O3	-0.1671	0.9410	0.5633	0.0120
O4	0.0125	0.7502	0.7101	0.0120
$O_5$	0.3689	0.4511	0.6001	0.0120
O6	0.4302	-0.0191	0.6054	0.0120
O7	0.6034	0.3036	0.5603	0.0121
O8	0.6046	0.2621	0.7143	0.0120
O9	0.2393	0.2301	0.7420	0.0260
H1	-0.1010	0.8180	0.7211	0.0500
H2	0.6621	0.0758	0.7322	0.0500
H3	0.3041	0.0810	0.6704	0.0500
H4	0.2122	0.2241	0.6703	0.0500

Table 6 Selected bond distances in Å.

	α−ZrP	$\alpha$ -TiP	$\alpha$ -HfP
Me-O1	2.042(2)	2.275(3)	2.068(2)
Me-O2	2.079(2)	2.234(3)	2.030(2)
Me-O5	2.058(2)	2.221(3)	2.046(2)
P1-O1	1.501(2)	1.502(3)	1.501(2)
P1-O2	1.512(2)	1.653(3)	1.515(2)
P1-O3	1.523(2)	1.632(3)	1.578(2)
P1-O4	1.565(2)	1.668(3)	1.502(2)
P2-O5	1.517(2)	1.671(3)	1.537(2)
P2-O6	1.517(2)	1.541(3)	1.582(2)
P2-O7	1.552(2)	1.547(3)	1.561(2)
P2-O8	1.519(2)	1.547(3)	1.535(2)
O4-H1	0.922(2)	0.828(3)	0.924(2)
O9-H1	1.568(2)	1.612(3)	1.544(2)
O7-H2	0.603(2)	0.690(3)	0.656(2)
О9-Н3	0.663(2)	0.681(3)	0.665(2)
O9-H4	1.038(2)	1.053(3)	1.037(2)

Remark: Me = Zr, Ti, and Hf, respectively

	$\alpha$ - <b>Z</b> r <b>P</b>	Angle in $^{\circ}$ $\alpha$ - <b>TiP</b>	α-HfP
O2 – Me* - O1	91.65 (8)	92.38 (8)	91.59 (6)
$\mathrm{O2-Me^*}$ - $\mathrm{O5}$	89.64 (7)	85.08(8)	99.05(6)
Me* - O2 - P1	148.56 (1)	143.78(2)	148.63(1)
O1 - P1 - O2	117.43 (1)	112.08(3)	117.98(1)
O1 - P1 - O3	110.47(2)	106.55(4)	109.89(3)
O1 - P1 - O4	109.12 (2)	120.67(3)	105.23(6)
O5 - P2 - O6	110.47(3)	109.44(3)	108.71(3)
O5 - P2 - O7	109.17(2)	120.67(5)	108.37(3)
P1 - O4 - H1	112.15(2)	110.71(3)	110.69(4)
P2-O7-H2	120.19 (3)	128.46(6)	118.00(3)
H3 - O9 - H4	114.97(3)	113.69(5)	114.31(3)

Table 7 Selected bond angles.

Remark\*: Me- = Zr, Ti, Hf, respectively

P-OH group was found to be  $23.92 \times 10^4$  pm<sup>2</sup>. This value showed a good agreement with that published by Clearfield and Costantino [14].

The modelling was based on the following basic structural data:

Space group: P 1 2 1/c1

Setting: monoclinic

Laue group: 2/m unique axis b

Point group: 2/m

Positions: 4e x, y, z; -x+1/2, y+1/2, -z+1/2; -x, -y-, -z; -x+1/2, -y+1/2, z+1/2;

001 projection of  $\alpha$ -HfP structure is illustrated on Fig. 2

#### 3.1.2 First-row divalent metal containing M<sup>4+</sup> phosphates

In the first step the XRPD patterns of transition metal containing phosphates were compared with that of the corresponding pure  $\alpha$ -forms. During the comparison the most striking difference found was the appearance of a new peak around the  $2\Theta \approx 10^{\circ}$  region. It was found that the intensity of this peak is increased by increasing the period of ion exchange process. In most cases the 002 peaks have maximum intensity in the diffraction patterns of transition metal containing samples. Consequently, it's relative occurrence can be used for analytical purpose in a multiphase system. The ratios between the relative intensity of peaks in 002 position of pristine phosphates and their transition metal containing forms were compared, and the data are presented in Table 8.

These data can be indicative for the estimation of the occurrence of the pristine phase in a mixture with the transition metal containing forms. The found values were in good correlation with analytical data, which we obtained after 200 hours digestion time (see Table 1). This can confirm that the investigated transition metal ions are built in the

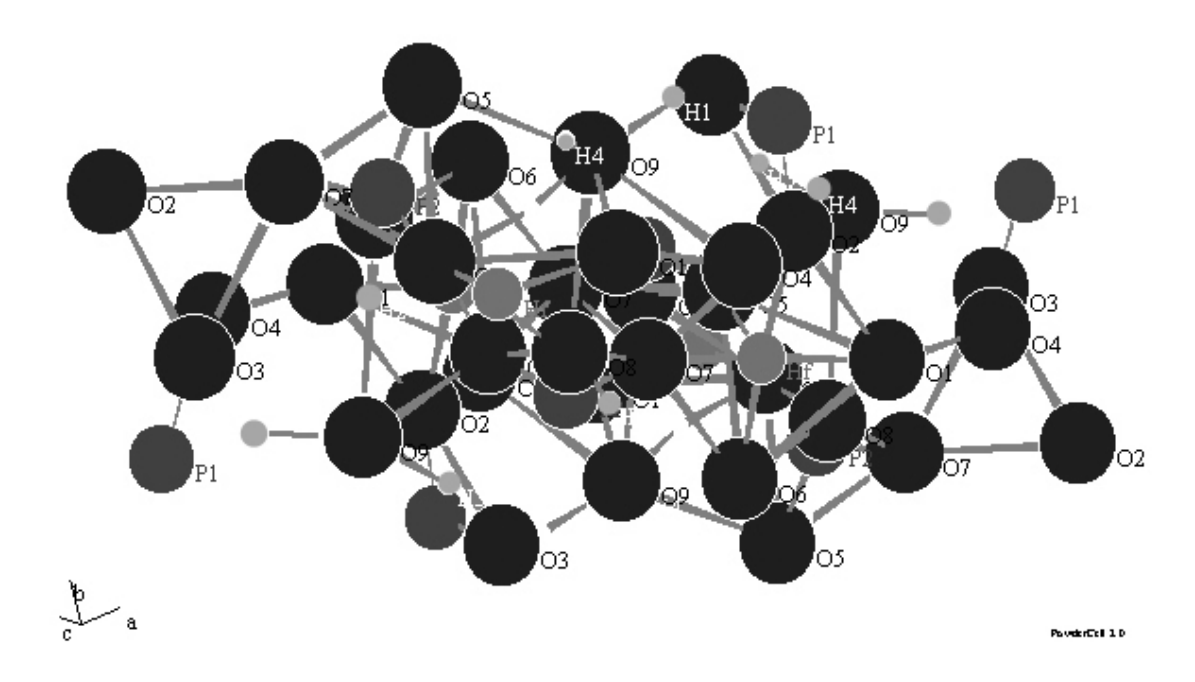


Fig. 2 The 001 projection of  $\alpha$ -hafnium phosphate structure.

**Table 8** Ratio of relative intensity between peaks of 002 position of pristine phosphates and their transition metal containing forms.

	Co (II)	Ni (II)	Mn (II)	Cu (II)	Zn (II)
$\alpha$ -ZrP	0.35	0.28	0.27	0.26	0.27
$\alpha$ -TiP	0.20	0.25	0.18	0.17	0.18
$\alpha$ -HfP	0.33	0.30	0.23	0.25	0.26

tetravalent metal phosphate structure.

Other data exhibited that, in case of higher than 70% loading, a single crystalline phase system occurs. This observation showed suitable similarities with the results presented by Clearfield and Kalnins [32]. According to above data, the prepared samples (with less than 70% loading) were two phase systems from crystallographic point of view. The forthcoming X-ray studies, however, are relating to samples having higher than 70% loading.

X-ray diffraction patterns of zirconium-, and titanium phosphates in form of fully loaded with transition metal ions, were published previously [33, 34]. Therefore, in this paper, only the fragment of XRPD pattern of transition metal containing  $\alpha$ -HfP is presented on Fig. 3.

On the diffraction patterns of transition metal containing phosphates (with different loading) can be seen among the positions and intensities of the lines. They can be explained by changing of lattice parameters, as well as the atomic scattering factors, for the different transition metals. The measured and calculated patterns show a good agreement to each other.

For all these XRPD patterns, the optimum evaluation was found when the monoclinic form was considered with the  $P_{12}$  space group. Taking into consideration these symmetrical conditions the XRPD patterns were calculated and compared (50 Bragg peaks) with those obtained experimentally. From this followed the determination of unit cell parameters shown in Table 9.

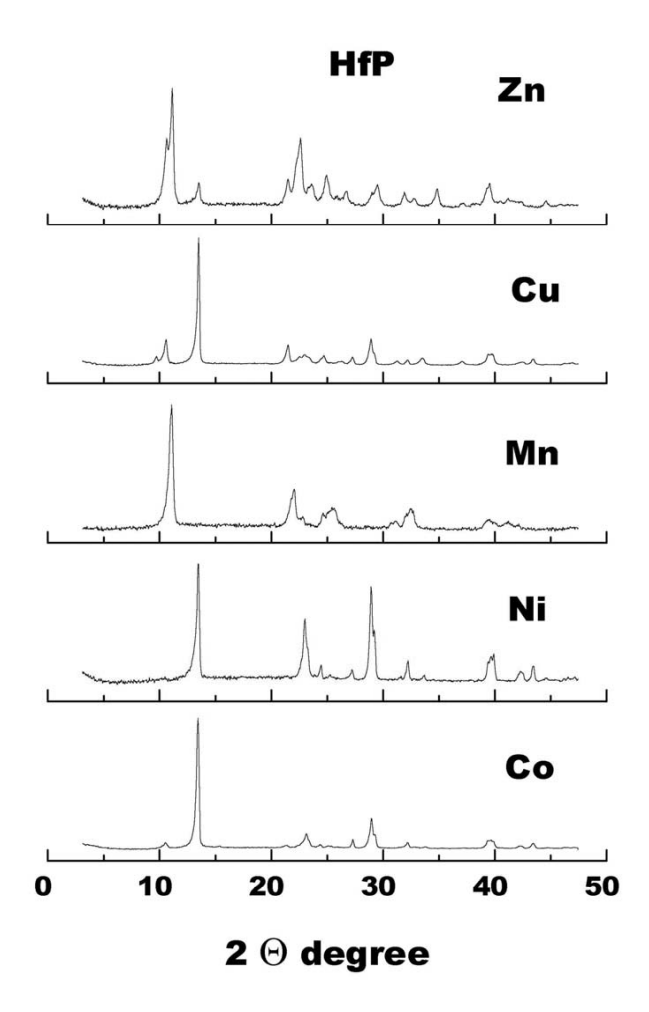


**Fig. 3** A fragment of XRPD patterns of transition metal containing  $\alpha$ -hafnium phosphates.

During the evaluation of the results collected in Table 9, we found for  $\alpha$ -ZrP the smallest difference in values of "a" axis which occur between the samples containing Co and Cu ( $\sim$ 0.1 Å). In the case of other transition metal ions, the difference does exceed the mentioned value, while for the "b" axis the difference among the investigated transition metal ions does not exceed about 0.2 Å. For "c" axis of  $\alpha$ -ZrP, a difference of  $\sim$  1.8 Å was found between the samples containing Co and Mn ions, while among the other samples containing Ni, Cu and Zn ions, differences of only  $\sim$ 0.3 Å were detected. The biggest change in d<sub>002</sub> values (0.13 Å) was found between the  $\alpha$ -ZrP samples containing Zn and Ni ions. Moreover a variation of  $\sim$ 1.9° in  $\beta$  was found among the various samples. For  $\alpha$ -TiP samples, significant changes were found in many cell parameters. Namely, the value of "a" axis in the case of Co- and Zn- containing samples differ on  $\sim$ 2.7 Å, at

Table 9 Unit cell parameters of transition metal containing tetravalent metal phosphates.

$\begin{array}{ c c c c c c c }\hline & & & & & & & & & & & & & & & & & & &$						
$\begin{array}{c ccccccccccccccccccccccccccccccccccc$		Co (II)				Zn (II)
$\begin{array}{c ccccccccccccccccccccccccccccccccccc$	. • .	` ′	. ,		<u> </u>	
$\begin{array}{c ccccccccccccccccccccccccccccccccccc$		` '	` '	` /	` '	( )
$\begin{array}{c ccccccccccccccccccccccccccccccccccc$	`	` ′	` ′	` '	`	` '
$\begin{array}{c ccccccccccccccccccccccccccccccccccc$	• •	` '	` '	` '	` '	` ,
$\begin{array}{c ccccccccccccccccccccccccccccccccccc$	'	103.21(2)	103.18(2)	` /	101.35(2)	103.26(2)
$ \begin{array}{c ccccccccccccccccccccccccccccccccccc$		9.551	9.642	9.587	9.590	9.511
$\begin{array}{c ccccccccccccccccccccccccccccccccccc$	Vol. $(\mathring{A}^3)$	938.89(6)	928.69(6)	877.15(7)	903.98(5)	914.78(6)
$\begin{array}{c ccccccccccccccccccccccccccccccccccc$	Rel. mass	1277.21	1394.06	1421.95	1385.86	1342.34
$\begin{array}{c ccccccccccccccccccccccccccccccccccc$	Atoms in	60.0	64.0	64.0	60.0	60.0
$\begin{array}{c ccccccccccccccccccccccccccccccccccc$	X-ray density (g.cm <sup>-3</sup> )	2.2589	2.4926	2.6919	2.5457	2.4366
$\begin{array}{c ccccccccccccccccccccccccccccccccccc$	Mass abs. coeff. $(cm^2.g^{-1})$	103.23	96.11	146.45	99.70	105.61
a (Å)			α-Ti	tanium phosp	phate	
$\begin{array}{c ccccccccccccccccccccccccccccccccccc$		Co (II)	Ni (II)	Mn (II)	Cu (II)	Zn (II)
$\begin{array}{c ccccccccccccccccccccccccccccccccccc$	a (Å)	10.722(3)	9.944(3)	9.296(4)	9.333(3)	8.037(3)
$\begin{array}{c ccccccccccccccccccccccccccccccccccc$	b (Å)	5.407(5)	5.556(6)	5.519(6)	5.557(5)	5.556(6)
$\begin{array}{c ccccccccccccccccccccccccccccccccccc$	c (Å)	24.611(2)	19.778(3)	21.556(3)	25.500(2)	23.981(2)
$\begin{array}{c ccccccccccccccccccccccccccccccccccc$	$eta^{\circ}$	106.80(3)	105.31(3)	104.65(3)	103.33(3)	104.42(3)
$\begin{array}{c ccccccccccccccccccccccccccccccccccc$	$d_{002}$ (Å)	11.409	9.604	10.220	12.596	11.994
$\begin{array}{c ccccccccccccccccccccccccccccccccccc$	0	1366.07(8)	1054.13(8)	1070.32(8)	1287.07(8)	1037.41(8)
X-ray density(g.cm <sup>-3</sup> ) 1.3043 1.8757 1.8517 1.5773 1.9454 Mass abs. coeff.(cm <sup>2</sup> .g <sup>-1</sup> ) 104.24 95.73 157.73 96.67 100.19 $ \frac{\alpha - \text{Hafnium phosphate}}{\alpha - \text{Hafnium phosphate}} $ Co (II) Ni (II) Mn (II) Cu (II) Zn (II) $ \frac{\alpha \text{ (Å)}}{\beta - \beta -$	Rel. mass	1072.97	1190.75	1193.57	1222.58	1215.403
Mass abs. coeff.(cm².g⁻¹)         104.24         95.73         157.73         96.67         100.19           α-Hafnium phosphate           Co (II)         Ni (II)         Mn (II)         Cu (II)         Zn (II)           a (Å)         9.276(1)         9.223(1)         9.217(2)         8.986(1)         8.623(1)           b (Å)         5.408(4)         5.537(4)         5.580(4)         5.537(4)         5.594(3)           c (Å)         19.826(3)         19.888(2)         18.928(3)         19.768(3)         18.899(2)           β°         101.33(2)         101.14(2)         101.18(2)         101.16(2)         101.31(2)           d <sub>002</sub> (Å)         9.737         9.760         9.755         9.690         9.714           Vol (ų)         975.18(7)         996.66(7)         955.36(7)         964.49(7)         893.97(7)           Rel. mass         1642.50         1642.15         1681.41         1742.44         1748.06           Atoms in         60.0         60.0         60.0         60.0         60.0           X-ray density (g ·cm⁻³)         2.7969         2.7360         2.9225         2.9999         3.2470	Atoms in	60.0	64.0	60.0	60.0	60.0
$\begin{array}{c ccccccccccccccccccccccccccccccccccc$	X-ray density(g.cm <sup>-3</sup> )	1.3043	1.8757	1.8517	1.5773	1.9454
$\begin{array}{c ccccccccccccccccccccccccccccccccccc$	Mass abs. coeff.( $cm^2.g^{-1}$ )	104.24	95.73	157.73	96.67	100.19
a (Å) $9.276(1)$ $9.223(1)$ $9.217(2)$ $8.986(1)$ $8.623(1)$ b (Å) $5.408(4)$ $5.537(4)$ $5.580(4)$ $5.537(4)$ $5.594(3)$ c (Å) $19.826(3)$ $19.888(2)$ $18.928(3)$ $19.768(3)$ $18.899(2)$ $\beta^{\circ}$ $101.33(2)$ $101.14(2)$ $101.18(2)$ $101.16(2)$ $101.31(2)$ $d_{002}$ (Å) $9.737$ $9.760$ $9.755$ $9.690$ $9.714$ Vol (ų) $975.18(7)$ $996.66(7)$ $955.36(7)$ $964.49(7)$ $893.97(7)$ Rel. mass $1642.50$ $1642.15$ $1681.41$ $1742.44$ $1748.06$ Atoms in $60.0$			α-Н	afnium phosp	hate	
$\begin{array}{c ccccccccccccccccccccccccccccccccccc$		Co (II)	Ni (II)	Mn (II)	Cu (II)	Zn (II)
$\begin{array}{c ccccccccccccccccccccccccccccccccccc$	a (Å)	9.276(1)	9.223(1)	9.217(2)	8.986(1)	8.623(1)
c (Å) $19.826(3)$ $19.888(2)$ $18.928(3)$ $19.768(3)$ $18.899(2)$ $\beta^{\circ}$ $101.33(2)$ $101.14(2)$ $101.18(2)$ $101.16(2)$ $101.31(2)$ $d_{002}$ (Å) $9.737$ $9.760$ $9.755$ $9.690$ $9.714$ Vol (ų) $975.18(7)$ $996.66(7)$ $955.36(7)$ $964.49(7)$ $893.97(7)$ Rel. mass $1642.50$ $1642.15$ $1681.41$ $1742.44$ $1748.06$ Atoms in $60.0$ $60.0$ $60.0$ $60.0$ $60.0$ $60.0$ X-ray density (g·cm <sup>-3</sup> ) $2.7969$ $2.7360$ $2.9225$ $2.9999$ $3.2470$	b (Å)	5.408(4)	5.537(4)	5.580(4)	5.537(4)	5.594(3)
$\begin{array}{c ccccccccccccccccccccccccccccccccccc$		19.826(3)	19.888(2)	18.928(3)	19.768(3)	18.899(2)
Vol (ų)975.18(7)996.66(7)955.36(7)964.49(7)893.97(7)Rel. mass $1642.50$ $1642.15$ $1681.41$ $1742.44$ $1748.06$ Atoms in $60.0$ $60.0$ $60.0$ $60.0$ $60.0$ X-ray density (g ·cm $^{-3}$ ) $2.7969$ $2.7360$ $2.9225$ $2.9999$ $3.2470$		101.33(2)	101.14(2)	101.18(2)	101.16(2)	101.31(2)
Vol (ų)975.18(7)996.66(7)955.36(7)964.49(7)893.97(7)Rel. mass $1642.50$ $1642.15$ $1681.41$ $1742.44$ $1748.06$ Atoms in $60.0$ $60.0$ $60.0$ $60.0$ $60.0$ X-ray density (g ·cm $^{-3}$ ) $2.7969$ $2.7360$ $2.9225$ $2.9999$ $3.2470$	$d_{002} (\mathring{A})$	9.737	9.760	9.755	9.690	9.714
Rel. mass $1642.50$ $1642.15$ $1681.41$ $1742.44$ $1748.06$ Atoms in $60.0$ $60.0$ $60.0$ $60.0$ $60.0$ X-ray density (g ·cm $^{-3}$ ) $2.7969$ $2.7360$ $2.9225$ $2.9999$ $3.2470$	0	975.18(7)	996.66(7)	955.36(7)	964.49(7)	893.97(7)
X-ray density $(g \cdot cm^{-3})$ 2.7969 2.7360 2.9225 2.9999 3.2470	, ,	1642.50	1642.15	1681.41	1742.44	1748.06
	Atoms in	60.0	60.0	60.0	60.0	60.0
	X-ray density (g $\cdot$ cm <sup>-3</sup> )	2.7969	2.7360	2.9225	2.9999	3.2470
	Mass abs. coeff. $(cm^2 \cdot g^{-1})$	134.09	135.43	176.43	130.04	131.67

the constant value of the "b" axis. For the value of "c" axis, an increase on 0.1~Å for Zn-containing sample was observed. At the same time, the change in value of "c" axis

showed a scattering among 0.9-5.7 Å for other investigated samples containing various transition metals. The biggest change in  $d_{002}$  values was found. In Ni- (9.603 Å) and Cu- (12.596 Å) containing samples The maximum difference in  $\beta$  angle (3°) was found between the samples containing Cu and Co ions, respectively. In case of  $\alpha$ -HfP samples, all the changes in cell parameters showed big similarities with those of  $\alpha$ -ZrP.

Comparing the cell parameters of samples containing various transition metals with those of the corresponding pristine tetra-valence metal phosphates revealed a significant difference only in the values of the "c" axes. The difference is  $\sim 5$  Å,  $\sim 4\text{-}10$  Å and  $\sim 4$  Å in case of  $\alpha\text{-}ZrP$ ,  $\alpha\text{-}TiP$  and  $\alpha\text{-}HfP$ , respectively. An increase of 2° was found in  $\beta$  angle in case of  $\alpha\text{-}ZrP$  and  $\alpha\text{-}HfP$ . The samples of  $\alpha\text{-}TiP$  showed a different picture, i.e. an increase of  $\sim 2^\circ$ ,  $\sim 3^\circ$ ,  $\sim 4^\circ$  and  $\sim 5^\circ$  was found for samples containing Cu, Mn, Zn, Ni and Co, respectively. Because of the difference in diameters of hydrogen and the used transition metal ions, the  $d_{002}$  values are increased. It was found that this increase is  $\sim 2$  Å for the samples of  $\alpha\text{-}ZrP$  and  $\alpha\text{-}HfP$ , respectively. In the case of the  $\alpha\text{-}TiP$  samples, the same increases are different; i.e. 2 Å for Ni,  $\sim 3$  Å, for Mn,  $\sim 4$  Å for Co and Zn, and  $\sim 5$  Å for Cu ion containing samples.

As an example, the difference plots of manganese containing ZrP, TiP and HfP (in  $\alpha$ -form) after refinement are presented on Fig. 4.

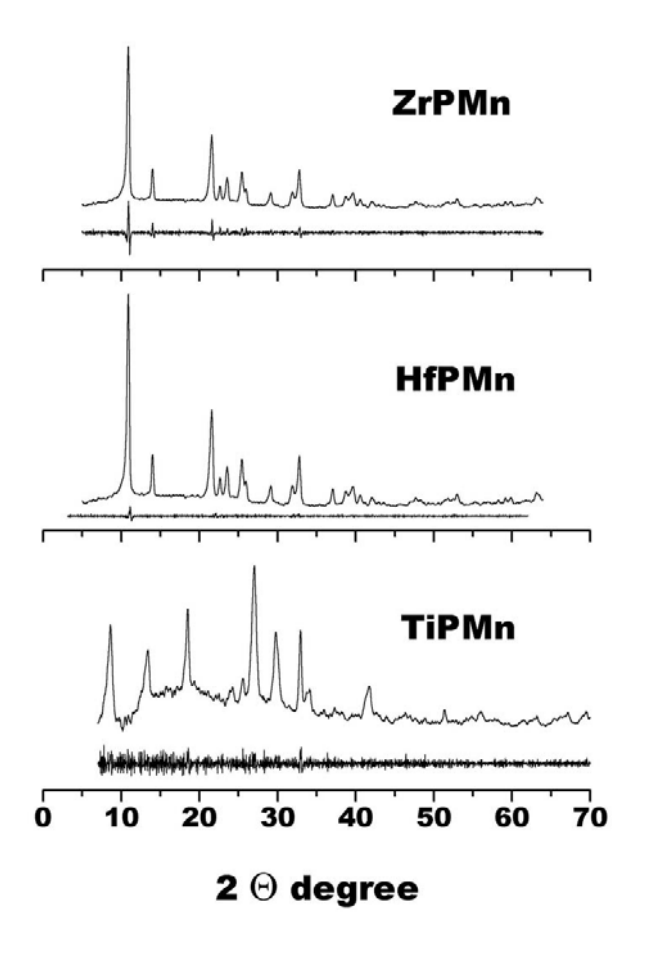


Fig. 4 The difference plot of Mn(II) containing phosphates (measured and calculated).

**Table 10** The positional and thermal parameters of Mn(II) containing metal(IV) phosphates.

		$\alpha ext{-}\mathrm{ZrP}$					$\alpha$ -TiP					$\alpha$ -HfP		
atom	×	y	Z	$\mathrm{B}_{iso}$	atom	×	y	Z	$\mathrm{B}_{iso}$	atom	×	y	Z	$\mathrm{B}_{iso}$
Zr	0.3461	0.4526	0.4051	0.425	$T_{\rm i}$	0.2350	0.2420	0.5180	0.419	JH	0.2461	0.2526	0.4851	0.019
P1	0.3874	0.7508	0.3857	0.531	P1	0.3690	0.7190	0.3220	0.529	P1	0.3874	0.7508	0.3857	0.081
P2	-0.1342	0.2420	0.3966	0.494	P2	-0.1470	0.2950	0.3970	0.529	P2	-0.1342	0.2420	0.3966	0.081
01	0.5445	0.8037	0.4374	0.622	01	0.5100	0.8610	0.5620	0.621	01	0.5445	0.8037	0.4374	0.126
02	0.3353	0.4862	0.4007	1.604	02	0.3660	0.4860	0.4010	1.603	02	0.3353	0.4862	0.4007	0.124
03	0.2772	0.9480	0.4065	0.816	03	0.2310	0.9410	0.3890	0.810	03	0.2772	0.9480	0.4065	0.125
04	0.3885	0.7559	0.2843	2.080	04	0.4040	0.7600	0.3160	2.049	04	0.3885	0.7559	0.2843	0.125
05	-0.2180	0.4364	0.4404	1.230	05	-0.2440	0.4330	0.4620	1.233	05	-0.2180	0.4364	0.4404	0.124
90	-0.1554	-0.0205	0.4316	1.131	90	-0.1180	-0.0240	0.4690	1.290	90	-0.1554	-0.0205	0.4316	0.126
07	-0.1942	0.2493	0.2949	1.171	07	-0.2250	0.2440	0.2900	1.168	07	-0.1942	0.2493	0.2949	0.125
08	0.0320	0.3070	0.4086	0.443	80	0.0510	0.3030	0.4050	0.442	80	0.0320	0.3070	0.4086	0.312
60	0.0042	0.7241	0.2617	1.954	60	0.0520	-0.2450	0.4070	1.953	60	0.0042	0.7241	0.2617	0.985
H3	0.0430	0.8150	0.2470	2.900	H3	0.0560	-0.1550	0.4060	2.900	H3	0.0430	0.8150	0.247	0.005
H4	0.0270	0.7010	0.3300	1.300	H4	0.0481	-0.2730	0.4020	1.300	H4	0.0370	0.7710	0.3300	0.005
Mn	0.0763	0.3620	0.2721	0.006	Mn	0.5112	0.2365	0.8830	0.511	Mn	0.0763	0.4620	0.2721	0.005

 $\textbf{Table 11} \ \text{Selected bond distances of transition metal containing phosphates in $\mathring{A}$.}$ 

		$\alpha ext{-}\mathbf{ZrP}$	rP					lpha-TiP					$\alpha$ -HfP		
	Co	Ż	m Mn	Cu	Zn	Ço	Ņ	m Mn	Cu	Zn	Co	Ņ	Mn	Cu	Zn
Me-O1	2.379(3)	2.379(3)	2.379(3)	2.379(3)	2.380(3)	1.783(5)	1.801(5)	1.804(5)	1.806(5)	1.741(5)	2.248 (3)	2.249(3)	2.250(3)	2.243(3)	2.253(3)
Me-O2	2.269(3)	2.257(3)	2.268(3)	2.268(3)	2.260(3)	1.757(5)	1.761(5)	1.791(5)	1.806(5)	1.787(5)	2.371(3)	2.387(3)	2.331(3)	2.371(3)	2.308(3)
Me-O5	2.211(3)	2.208(3)	2.213(3)	2.209(3)	2.211(3)	2.500(5)	2.560(5)	2.566(5)	2.559(5)	2.564(5)	2.287(3)	2.319(3)	2.282(3)	2.312(3)	2.281(3)
Me(II)-O4	1.960(3)	1.781(3)	1.781(3)	1.264(3)	0.840(3)	1.744(5)	1.899(5)	2.023(5)	2.072(5)	1.872(5)	1.672(3)	1.725(3)	1.310(3)	1.254(3)	0.961(3)
P1-01	1.731(3)	1.510(3)	1.580(3)	1.510(3)	1.510(3)	1.790(5)	1.844(5)	1.800(5)	1.806(5)	1.797(5)	1.634(3)	1.634(3)	1.611(3)	1.599(3)	1.526(3)
P1-O2	1.529(3)	1.512(3)	1.525(3)	1.512(3)	1.512(3)	1.862(5)	1.775(5)	1.858(5)	1.802(5)	1.721(5)	1.557(3)	1.588(3)	1.595(3)	1.584(3)	1.588(3)
P1-O3	1.570(3)	1.523(3)	1.554(3)	1.523(3)	1.523(3)	1.691(5)	1.795(5)	1.767(5)	1.783(5)	1.786(5)	1.587(3)	1.599(3)	1.597(3)	1.582(3)	1.556(3)
P1-04	1.528(3)	1.565(3)	1.569(3)	1.565(3)	1.565(3)	1.930(5)	1.647(5)	1.892(5)	1.653(5)	1.651(5)	1.512(3)	1.519(3)	1.521(3)	1.507(3)	1.518(3)
P2-O5	1.510(3)	1.517(3)	1.518(3)	1.517(3)	1.517(3)	1.685(5)	1.608(5)	1.642(5)	1.61(5)	1.620(5)	1.652(3)	1.666(3)	1.645(3)	1.652(3)	1.620(3)
P2-O6	1.517(3)	1.51(3)	1.512(3)	1.518(3)	1.517(3)	1.752(5)	1.737(5)	1.987(5)	1.881(5)	1.686(5)	1.609(3)	1.639(3)	1.635(3)	1.637(3)	1.635(3)
P2-O7	1.955(3)	1.852(3)	1.841(3)	1.852(3)	1.852(3)	1.857(5)	1.925(5)	1.766(5)	2.175(5)	1.872(5)	1.984(3)	1.992(3)	1.898(3)	1.977(3)	1.890(3)
P2-08	1.625(3)	1.625(3)  1.519(3)  1.532(3)  1.519(3)	1.532(3)	1.519(3)	1.519(3)	1.749(5)	1.722(5)	1.753(5)	1.772(5)	1.771(5)	1.553(3)	1.441(3)	1.455(3)	1.433(3)	1.453(3)

Remark: Me = Zr, Ti, Hf, respectively; Me(II) = Co, Ni, Mn, Cu, Zn, respectively

Table 12 Selected bond angles of transition metal containing Me(IV) phosphates.

			)				)			
					Angle in °	o in e				
	Co	Ni	$lpha ext{-ZrP}$ Mn	Cu	Zn	Co	Ni	$lpha ext{-TiP}$	Cu	Zn
O2-Me*-O1	98.40 (3)	97.99(3)	97.59(4)	98.01(3)	97.99(4)	95.38(5)	97.68(4)	93.38(3)	93.12(5)	92.70(3)
$O2-Me^*-O5$	97.25 (3)	96.48(3)	96.32(3)	97.11(2)	96.48(4)	94.40(5)	96.94(5)	92.82(2)	92.55(5)	92.01(3)
$Me^*-O2-P1$	142.29(3)	144.83(3)	144.70(3)	144.83(2)	144.83(3)	110.11(3)	117.48(5)	114.67(2)	115.12(3)	117.14(3)
O1-P1-O2	109.05(3)	112.43(2)	109.54(4)	112.43(2)	112.43(2)	110.72(2)	109.10(4)	112.35(4)	110.48(4)	110.21(3)
O1-P1-O3	108.61(3)	110.46(3)	106.63(3)	110.46(3)	110.46(3)	109.87(2)	110.11(3)	114.38(3)	115.57(3)	115.21(3)
O1-P1-O4	117.68(3)	109.12(3)	114.14(3)	109.12(3)	109.12(3)	116.88(4)	116.21(3)	113.76(3)	116.32(3)	116.11(5)
O5-P2-O6	104.90(3)	110.66(3)	109.32(2)	110.66(3)	110.66(3)	96.05(2)	96.06(4)	108.21(2)	98.74(5)	96.07(5)
O5-P2-O7	113.02(3)	109.17(3)	105.07(1)	109.17(3)	109.17(3)	95.66(4)	95.66(4)	98.28(4)	96.69(2)	95.62(3)
Н3-О9-Н4	120.80(3)	119.98(3)	118.47(3)	114.98(3)	114.98(3)	82.64(4)	82.74(4)	76.60(2)	75.45(4)	82.76(2)
$Me^{**}-06-P2$	112.09(3)	114.60(2)	150.59(2)	152.59(2)	143.31(3)	130.81(4)	130.65(2)	133.55(2)	137.53(4)	129.41(4)
			Angle in $^{\circ}$							
	Co	Ni	Mn	Cu	Zn					
O2-Me*-O1	100.37(4)	100.97(2)	98.98(4)	101.89(3)	102.01(4)					
$O2-Me^*-O5$	99.43(2)	98.22(3)	95.46(4)	97.83(3)	94.87(4)					
$\mathrm{Me}^*$ -O2-P1	161.72(2)	161.30(3)	160.89(2)	160.91(1)	159.93(4)					
O1-P1-O2	108.24(2)	108.12(3)	109.13(3)	107.82(3)	108.13(3)					
O1-P1-O3	105.07(2)	104.21(3)	105.30(2)	103.10(3)	102.06(3)					
O1-P1-O4	116.45(4)	116.86(2)	115.28(3)	117.34(2)	117.13(2)					
O5-P2-O6	102.99(2)	104.23(3)	106.39(2)	104.72(1)	107.43(4)					
O5-P2-O7	117.03(4)	116.86(3)	115.05(2)	114.64(3)	116.39(3)					
Н3-О9-Н4	82.97(3)	82.96(3)	82.72(3)	82.90(2)	82.96(2)					
$\mathrm{Me}^{**}$ -O6-P2	120.92(3)	111.25(3)	118.25(2)	118.32(2)	122.29(2)					

Remark:  $Me^* = Zr$ , Ti, Hf, respectively;  $Me^{**} = Co$ , Ni, Mn, Cu, Zn, respectively

Using the same basic data mentioned above for  $\alpha$ -HfP, the structure of the prepared materials were modelled. As an example the 001 projection of Mn(II) containing  $\alpha$ -HfP is shown in Fig. 5. The resulting positional and thermal parameters are collected in Table 10, while the selected bond distances and bond angle data are given in Tables 11 and 12, respectively.

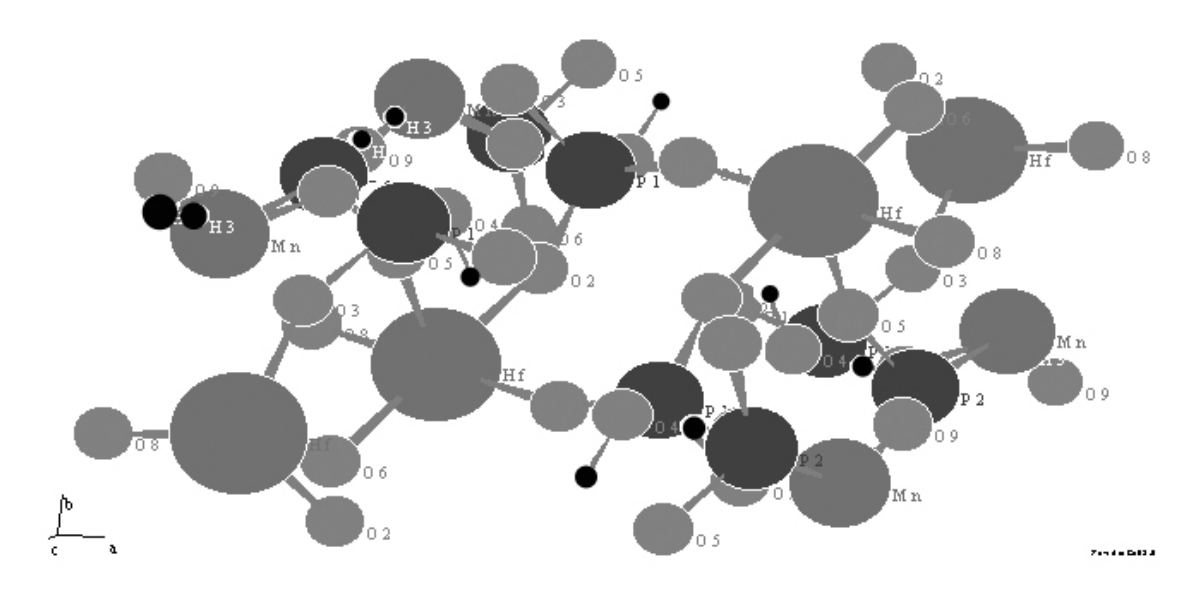


Fig. 5 The 001 projection of Mn(II) containing  $\alpha$ -hafnium phosphate structure.

It was found that all atomic distances and angles and also the temperature factors showed no anomalous discrepancies.

### 4 Summary

In evaluating the bond distance data (Me-O1) of transition metal containing phosphates, practically no difference was found between the samples containing various transition metals. An exception was found for  $\alpha$ -TiP samples.In this case, the bond distance values are increasing with max. 0.04 Å in the direction of Zn – Co containing samples. When these data are compared with that of the pristine tetravalent metal phosphates, no difference was found among them for  $\alpha$ -ZrP and  $\alpha$ -HfP, while for the  $\alpha$ -TiP samples the same data are about 0.6 Å less than those for pristine  $\alpha$ -TiP.

When comparing the data of various phosphates in more detail, the O-H bonds showed nearly identical value except those of titanium phosphate, where the bonds were found to be about 0.2 Å shorter than those for the other investigated phosphates. The Me-O bonds (where Me = Zr,Ti and Hf, respectively) showed various character. For example, the Me-O2 bond for hafnium phosphate was found to be longer than those for the other phosphates. At the same time the Me-O6 bond was found the same for all three investigated phosphates. The various P-O bonds, vary between 1.58 - 2.04 Å and showed the same values for all three investigated phosphates. Comparing these values with those of pristine phosphates for example, in case of  $\alpha$ -ZrP the bond length for transition metal

forms was generally found to be  $\sim 0.04$  Å longer. In case of  $\alpha$ -TiP, this value reached the 0.05 Å, while in case of  $\alpha$ -HfP, it was found  $\sim 0.4$  Å. Evaluating the bond angle results did not reveal any considerable difference between the data of pristine tetravalent metal phosphates and their transition metal containing forms.

From the XRPD pattern analysis, it was found that the "c" axis of the unit cell is increased after the finishing of the ion exchange process, while the other lattice parameters and the angle generally have an insignificant change. The interlayer distances significantly increased corresponding to the atomic diameters [35] of given transition metal ions, which were placed between the layers. This increase only partly follows the real increasing of diameters of the given transition metal ions. It seems that the increase of interlayer distance depends more on the rate of quantity of given transition metal ions up taken by tetravalent metal phosphates. These facts caused insignificant distortion in the Me<sup>4+</sup>-O bond distances, without changing the structure.

Taking into consideration the above data, it can be proposed that the transition metal containing zirconium-, titanium- and hafnium phosphates have the same layered structure as the corresponding pristine phosphates. The fact that the transition metals changed place with hydrogen ions caused some distortion also in some O-H bonds.

#### 5 Conclusion

Using the ion exchange method the first-row transition metal containing zirconium-, titanium-, and hafnium phosphates were prepared. Using equilibration of the given solutions at 80°the total exchange of protons for transition metals cannot be attainable. The analytical data confirmed that the transition metal ions are changed in non-hydrated form.

As a result of XRPD analysis, it was found that the structure of titanium and hafnium phosphates are isomorphous. Their transition metal containing forms also have layered monoclinic structure. As a result of ion exchange, the interlayer distance and the "c" axis of the unit cell is increased and the change of hydrogen- for transition metal ions caused some distortion inside the layer due to the change of some bond distances between the Me<sup>4+</sup> and O and some O-H bonds. The samples containing various transition metals did not show great differences.

# Acknowledgment

The support from Hungarian OTKA Fund (M-027367 and No 043687) is greatly appreciated.

#### References

[1] I.V. Tanaev (Ed.): The Chemistry of Tetravalent Elements Phosphates, Nauka, Moscow 1972 and references therein.

- [2] M.T. Averbuch-Pouchot and A. Durif (Eds.): *Topics in Phosphate Chemistry*, World Sci, Singapore, 1994.
- [3] A. Clearfield and J.A. Stynes: "The preparation of crystalline zirconium phosphate and some observation on its ion exchange behaviour", *J. Inorg. Nucl. Chem.*, Vol. 26, (1964), pp. 117–129.
- [4] A. Clearfield and G.D. Smith: "The crystallography and structure of zirconium bis(monohydrogen orthophosphate) monohydrate", *Inorg. Chem.*, Vol. 8, (1969), pp. 431–436.
- [5] G. Alberti and E. Torracca: "Crystalline insoluble acid salts of polyvalent metals and polybasic acids VI", *J. Inorg. Nucl. Chem.*, Vol. 30, (1968), pp. 3075–3080.
- [6] L. Szirtes: Investigation on zirconium phosphate ion exchange material, Thesis (Ph.D), Moscow State University, Moscow, 1968 (in Russian).
- [7] S. Bruque, M.A.G. Aranda, E.R. Losilla, P. Olivera-Pastor and P. Maireles-Tores: "Synthesis, optimisation and crystal structures of layered metal(IV) hydrogen phosphates", *Inorg. Chem.*, Vol. 34, (1995), pp. 893–899.
- [8] J.M. Troup and A. Clearfield: "On the mechanism of ion exchange in zirconium phosphate 20. Refinement on the crystal structure of α-zirconium phosphate", *Inorg. Chem.*, Vol. 16, (1977), pp. 3311–3314.
- [9] Tomita, K. Magami, H. Watanabe, K. Suzuki and T. Nakamura: "Single-step Lithium-ion Exchange on α-Hafnium Phosphate", Bull. Chem. Soc. Japan, Vol. 56, (1983), pp. 3183–3186.
- [10] L. Szirtes: "Progress in chemistry of inorganic ion exchangers", Thesis (D.Sc.), Hungarian Academy of Sciences Budapest, 1987 (in Hungarian).
- [11] A. Clearfield (Ed.): *Inorganic Ion Exchange Materials CRC Press*, Boca Raton, FL, 1982, Chp. 1, pp. 30,35 and references therein.
- [12] A. Clearfield: Progress in Intercalation Research, Kluwer Dordrecht, 1994, p. 223.
- [13] G. Alberti, C. Dionigi, S. Murcia-Mascaros and R. Vivani, In: G. Tsoucaris (Ed.): Crystallography of Supramolecular Compounds, Kluwer Dordrecht, 1996, p. 143.
- [14] A. Clearfield and U. Costantino: "Layered Metal Phosphates and Their Intercalation Chemistry", In: G. Alberti and T. Bein (Eds.): Comprehensive Supramolecular Chemistry, Pergamon Press, N.Y., 1996.
- [15] G.C. Hadjipanayis and R.W. Siegel (Eds): Nanophase Materials: Synthesis, Properties, Applications Kluwer Dordrecht, 1994, references therein.
- [16] G. Alberti, S. Cavalaglio, F. Marmottini, K. Matusek, J. Megyeri and L. Szirtes: "Preparation of a composite γ-zirconium phosphate-silica with large specific surface and its first characterisation as acid catalyst", Appl. Catal. A: General, Vol. 218, (2001), pp. 219–228.
- [17] V. Brandel and N. Dacheux: "Chemistry of tetravalent actinide phosphate part I", J. Solid State Chem., Vol. 177, (2004), pp. 4743–4754.
- [18] S.K. Shakshooki, N. Naqvi, J. Kowalczyk, S. Khalil, M. Rais and F. Tarish: "Mixed insoluble acid salts of tetravalent metals II", React. Polym., Vol. 7, (1988), pp. 221– 226.

- [19] S.K. Shakshooki Y. Elmismari, A. Dehair and L. Szirtes: "Mixed acid salts of tetravalent metals IX", J. Radioanal. Nucl. Chem. Art., Vol. 158, (1992), pp. 3–12.
- [20] S.K. Shakshooki, N. Naqvi, S. Khalil, M. Mostaq and L. Szirtes: "Mixed acid salts of tetravalent metals VI", J. Radioanal. Nucl. Chem. Art., Vol. 121(1), (1988), pp. 195–201.
- [21] S.K. Shakshooki, F. Masaodi, A. Dehair, J. Kowalczyk and L. Szirtes: "Mixed acid salts of tetravalent metals VIII", J. Radioanal. Nucl. Chem. Art., Vol. 132(2), (1989), pp. 251–260.
- [22] M. Suárez, L.M. Barcina, R. Llavona and J. Rodriguez: "Layered hafnium phosphates. Synthesis, characterisation, crystalline structure and intercalation behaviour", *J. Mol. Struct.*, Vol. 470, (1998), pp. 105–119.
- [23] L. Szirtes, J. Megyeri, L. Riess and E. Kuzmann: "Thermal decomposition of hafnium phosphate and related materials", *J. Therm. Anal. Cal.*, Vol. 65, (2001), pp. 975–981.
- [24] R.B. Sandell (Ed): Colorimetric Determination of Traces of Metals, Intersci. Publ. Inc., N.Y., 1959, pp. 426,453, 610, 674,870, 941, 966.
- [25] Z. Klencsár: *EXRAY*, peak searching computer software, Personal communication, 1998.
- [26] H.M. Rietveld: "Profile refinement method for nuclear and magnetic structures", *J. Appl. Crystallogr.*, Vol. 2, (1969), pp. 65–71.
- [27] W. Kraus and G. Nolze: *Powder Cell*, ver. 2.3 (software for structural simulation), 1999.
- [28] L. Szirtes. A.M. Szeleczky, A.O. Rajeh and E. Kuzmann: "Thermal behaviour of transition metal containing zirconium phosphate", J. Therm. Anal. Cal., Vol. 56, (1999), pp. 447–451.
- [29] L. Szirtes, L. Riess and J. Megyeri: "Thermal-analytical investigation of layered titanium salts", *J. Therm. Anal. Cal.*, Vol. 73, (2003), pp. 209–219.
- [30] L. Szirtes, L. Riess and J. Megyeri: "Thermoanalytical investigation of crystalline layered hafnium salts", *J. Therm. Anal. Cal.*, Vol. 79, (2005), pp. 135–140.
- [31] L. Zsinka and L. Szirtes: "Determination of specific surface of some synthetic ion exchangers; Measurements in gas and liquid phases", *Magy. Kém. Folyóirat*, Vol. 74(6), (1968), pp. 258–260 (in Hungarian).
- [32] A. Clearfield and J.M. Kalnins: "On the mechanism of ion exchange in zirconium phosphates XIII", *J. Inorg. Nucl. Chem.*, Vol. 38, (1976), pp. 849–852.
- [33] L. Szirtes, J. Megyeri, E. Kuzmann and Z. Klencsár: "Electrical conductivity of transition metal containing crystalline zirconium phosphate materials", *Solid State Ionics*, Vol. 145, (2001), pp. 257–260.
- [34] L. Szirtes, J. Megyeri, L. Riess and E. Kuzmann: "Electrical conductivity of transition metal containing crystalline titanium phosphate materials", *Solid State Ionics*, Vol. 162-163, (2003), pp. 181–184.
- [35] W. Hume-Rothery and G.V. Raynor: *The Structure of Metals and Alloys*, Ed. By Inst. Of Metals, London, 1954, pp. 100–103.